Ecological Processes

RESEARCH

Open Access

Large-diameter trees and deadwood correspond with belowground ectomycorrhizal fungal richness

Joseph D. Birch[1,2*], James A. Lutz[2], Soren Struckman[2], Jessica R. Miesel[1] and Justine Karst[3]

Abstract

Background: Large-diameter trees have an outsized influence on aboveground forest dynamics, composition, and structure. Although their influence on aboveground processes is well studied, their role in shaping belowground fungal communities is largely unknown. We sought to test if (i) fungal community spatial structure matched aboveground forest structure; (ii) fungal functional guilds exhibited differential associations to aboveground trees, snags, and deadwood; and (iii) that large-diameter trees and snags have a larger influence on fungal community richness than smaller-diameter trees. We used MiSeq sequencing of fungal communities collected from soils in a spatially intensive survey in a portion of Cedar Breaks National Monument, Utah, USA. We used random forest models to explore the spatial structure of fungal communities as they relate to explicitly mapped trees and deadwood distributed across 1.15 ha of a 15.32-ha mapped subalpine forest.

Results: We found 6,177 fungal amplicon sequence variants across 117 sequenced samples. Tree diameter, deadwood presence, and tree species identity explained more than twice as much variation (38.7% vs. 10.4%) for ectomycorrhizal composition and diversity than for the total or saprotrophic fungal communities. Species identity and distance to the nearest large-diameter tree (≥ 40.2 cm) were better predictors of fungal richness than were the identity and distance to the nearest tree. Soil nutrients, topography, and tree species differentially influenced the composition and diversity of each fungal guild. Locally rare tree species had an outsized influence on fungal community richness.

Conclusions: These results highlight that fungal guilds are differentially associated with the location, size, and species of aboveground trees. Large-diameter trees are implicated as drivers of belowground fungal diversity, particularly for ectomycorrhizal fungi.

Keywords: Belowground ecology, Ectomycorrhizal fungi, *Pinus flexilis*, *Pinus longaeva*, Saprotrophic fungi, Smithsonian ForestGEO, Spatial dynamics, Utah Forest Dynamics Plot

Background

Trees, snags, and deadwood interact directly and indirectly with fungi by providing resources aboveground and belowground and modifying the microenvironment (Smith and Read 2010). These interactions vary with tree species, size, age, and distance, which have all been implicated as influencing fungal community composition (Teste and Simard 2008; Birch et al. 2021). Tree species vary in the amount and nutrient content of their litterfall (Vogt et al. 1995; Keane 2008), root exudates (Vives-Peris et al. 2020), longevity, and life-history strategies, all of which can alter the environment and influence the assembly of fungal communities (Birch et al. 2022b). In addition to species identity, individual trees' size, location, and age can also influence fungal communities (Nguyen et al. 2016b; Rudawska et al. 2018; Wasyliw

*Correspondence: coope456@msu.edu

[1] Department of Plant, Soil and Microbial Sciences, Michigan State University, 1066 Bogue Street, East Lansing, MI 48824, USA
Full list of author information is available at the end of the article

Springer Open

© The Author(s) 2023. **Open Access** This article is licensed under a Creative Commons Attribution 4.0 International License, which permits use, sharing, adaptation, distribution and reproduction in any medium or format, as long as you give appropriate credit to the original author(s) and the source, provide a link to the Creative Commons licence, and indicate if changes were made. The images or other third party material in this article are included in the article's Creative Commons licence, unless indicated otherwise in a credit line to the material. If material is not included in the article's Creative Commons licence and your intended use is not permitted by statutory regulation or exceeds the permitted use, you will need to obtain permission directly from the copyright holder. To view a copy of this licence, visit http://creativecommons.org/licenses/by/4.0/.

and Karst 2020). Trees can also directly host symbiotic and saprotrophic fungi on and within their roots, and thus directly influence fungal communities (Smith and Read 2010). Because these tree-provided resources vary in quality and quantity, the aboveground structure and composition of forests likely influence the belowground community of fungi.

Large-diameter trees contain a disproportionate amount of aboveground biomass within forests (Lutz et al. 2018) and deadwood (Lutz et al. 2020, b). The largest trees may have a distinctive influence on belowground fungal community structure through greater root length and area (Bauhus 2009), higher respiration relative to photosynthesis (Tang et al. 2014), or through their longevity (Birch et al. 2021). The influence of a tree on the environment may decline with increasing distance, with the strength of the distance–decay relating to the size of the tree and the density of the surrounding forest. Thus, we expect that large-diameter trees might have a large influence on belowground fungal communities, even at great distances. Large-diameter trees could support unique fungal communities owing to specific fungi promoting greater growth and survival or because large-diameter trees select different fungi due to altered nutrient requirements and larger rooting extents that change with tree ontogenesis (Fig. 1). The greater resource requirements, rooting extents, and potential for differential bi-directional selection between fungi and large trees could conceivably select for different ectomycorrhizal fungal communities relative to small trees. Likewise, large-diameter trees are likely to release larger amounts of litterfall and necromass (Maguire 1994) relative to smaller trees which could support saprotrophic communities. In either case, we would expect that large-diameter tree location, size, and species may have consequences for belowground fungal communities.

The spatial extent over which fungal community composition is similar, i.e., autocorrelated, is important when parsing the abiotic drivers of plant composition and structure (Kim and Shin 2016), as the inclusion of spatial autocorrelation can improve identification of the environmental variables influencing communities. Likewise, understanding the drivers of forest and fungal community composition necessitates identification of the extent over which they vary in space. Many soil fungal communities are autocorrelated between 2–3 m, though some species can have spatial autocorrelation upward to 17 m, indicating large genets (Lilleskov et al. 2004; Boraks et al. 2021). Trees, deadwood, and abiotic variables, such as pH, vary with space (Lutz et al. 2013, 2021a), and if fungal communities are influenced by these features, we would expect congruent spatial autocorrelation between aboveground forest structure and belowground fungi. For example, the diversity of tree litter corresponds with

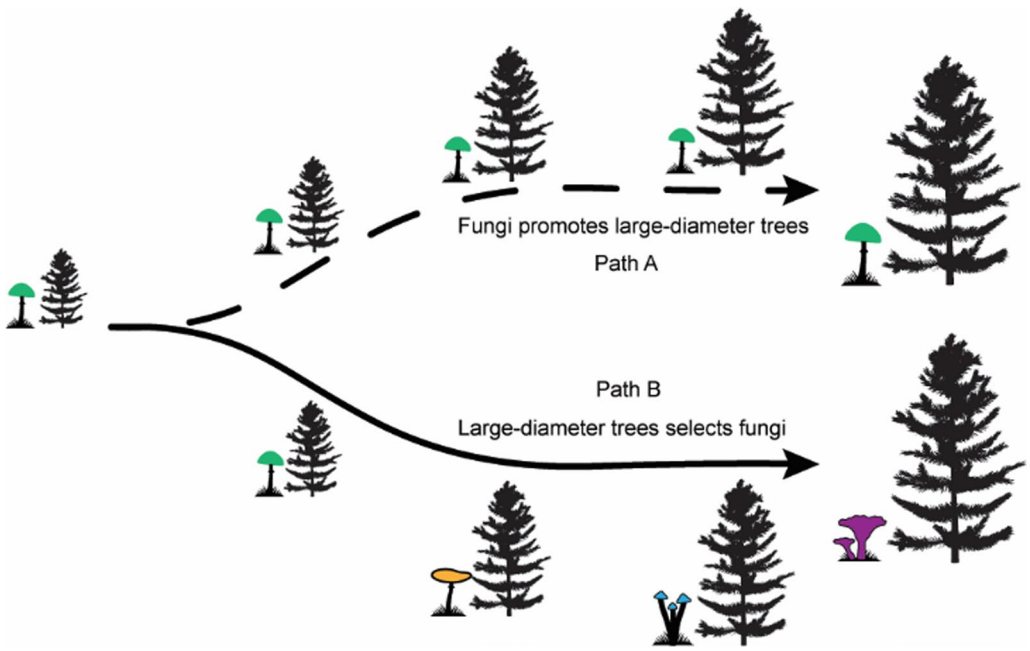

Fig. 1 Conceptual diagram of how fungi may promote (path A) or be selected by large-diameter trees (path B) with time. Under path A the same fungal community endures from tree recruitment to old-growth and promotes the tree survival and growth. Under path B the tree selects different fungal partners as it progresses from recruitment to old-growth

saprotrophic diversity and may alter saprotrophic community composition due to saprotroph specialization in species specific carbon and litter (Hanson et al. 2008; Otsing et al. 2018).

The subalpine forests of the southwestern United States represent a diverse and spatially isolated collection of mixed-conifer forests. These forests frequently encompass multiple coexisting overstory Pinaceae species as well as aspen and tall shrubs. Decomposition rates are slow, so deadwood remains for centuries (Kueppers et al. 2004). Through a spatially intensive survey of soil fungal communities, we sought to identify fungal communities in a high-elevation, old-growth forest. Specifically, we sought to test if (H1) fungal communities had spatial autocorrelations that closely matched aboveground forest structure, (H2) fungal functional guilds would exhibit differential associations to aboveground tree, snag, and downed wood structure, and (H3) that large-diameter tree and snags would have a larger influence on fungal community diversity than would smaller-diameter trees.

Methods

Site description

The study was located within the subalpine, mixed-conifer forest at the Utah Forest Dynamics Plot (UFDP) located within Cedar Breaks National Monument, Utah, USA (37.66°N, 112.85°W) (Fig. 2). The UFDP was established according to the protocols of the Smithsonian Forest Global Earth Observatory network (Davies et al. 2021) with all living and dead stems ≥ 1.0 cm diameter at breast height (DBH; 1.37 m) in 15.32 ha being identified, mapped and annually assessed for mortality (Lutz 2015). This survey included 25,478 living trees, 4400 snags, and 5,310 pieces of deadwood originating from the main stems of trees ≥ 10 cm diameter (Lutz et al. 2021a). The UFDP contains 11 overstory tree species with maximum species ages ranging from 220–1400 years old (Furniss et al. 2017; Birch et al. 2021). Deadwood was divided into five decay classes (Harmon et al. 2008). Species-specific tree-ring chronologies have been collected for all tree species within the UFDP with more than 15 individuals (Anderson-Teixeira et al. 2022).

We established a sampling grid within a 1.15-ha section of the UFDP characterized by a diverse, old-growth closed-canopy forest. We selected this area due to the diverse composition and structure of the aboveground forest and similarity in aspect across a contiguous area. This area spans an elevation of 3037–3089 m with a mean annual temperature of 3.9 °C and mean annual precipitation of 768 ± 119 mm, of which 506 ± 137 mm occurs as snow. Soils are categorized within the Mollisol (Argicryolls) and Inceptisol (Haplocryepts) orders and are alkaline (pH 7.0–8.1), calcareous, and have high base cation content. Soil textures within the sampling area are generally categorized as clay to clay loams.

The sampling area is composed of *Abies bifolia* A. Murray bis (Rocky Mountain subalpine fir), *Populus tremuloides* Michaux (quaking aspen), *Picea pungens* Engelmann (Colorado blue spruce), *Picea engelmannii* var. *engelmannii* Parry ex Engelmann (Engelmann spruce), *Pinus longaeva* D. K. Bailey (Great Basin bristlecone pine), and *Pinus flexilis* E. James (limber pine), with low abundances of *Pseudotsuga menziesii* var. *glauca* (Mayr) Franco (interior Douglas-fir), *Pinus ponderosa* Douglas ex Lawson & C. Lawson (ponderosa pine), *Abies concolor* (Gordon & Glendinning) Hildebrand (white fir), *Juniperus communis* Linnaeus (common juniper), and *Ribes cereum* Douglas (wax currant) in the adjoining forest (Additional file 1: Table S1) (Furniss et al. 2017). The forest has had no recorded management actions and has multiple cohorts originating from natural regeneration following patchy and infrequent high-severity fire with

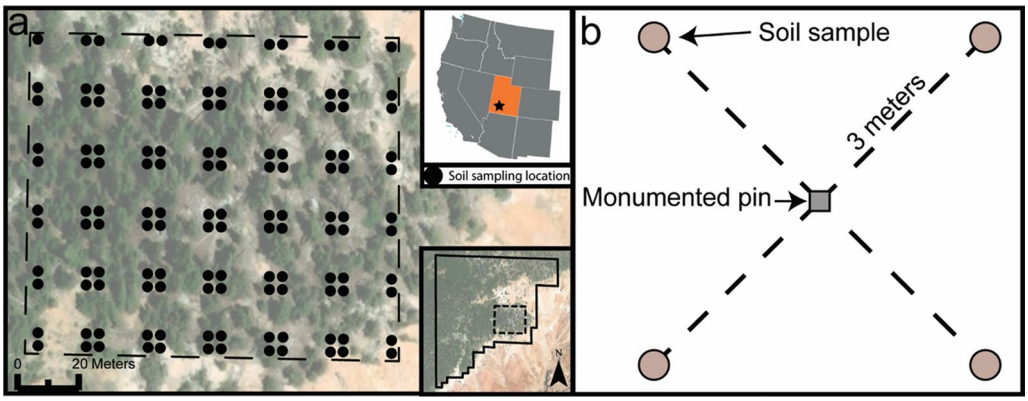

Fig. 2 The location of soil sampling (**a**) within the Utah Forest Dynamics Plot (UFDP), Utah, USA. Samples were taken 3 m away from monumented pins (**b**) placed within a 20 × 20 m grid at the UFDP

the most recent fire likely occurring in 1802 (Lutz et al. 2021a). Live tree ages in the dataset range from 2-year seedlings to 1400 years old (Birch et al. 2021). Characteristic disturbances include infrequent, high-severity fire, drought, bark-beetle outbreaks, high wind events, and growing season frost (Lutz et al. 2021a; Birch et al. 2022a). The 1.15-ha sampling area is structurally diverse (Fig. 3) with both small (< 5 m) and large (~ 10 m) canopy gaps distributed across the multiple cohorts of mixed conifers.

Belowground sampling

To sample fungi, we collected soil samples across a 115 × 100 m grid overlaid across the monumented 20 × 20 m grid present in the UFDP (Fig. 2a). We sampled at distances of 3.0 m from these grid-points at fixed azimuths of 45°, 135°, 225°, and 315° (Fig. 2b). We used a soil knife (Zenport; Sherwood, Oregon) to sample soil in a 4 × 4 cm area to a depth of 25 cm. We sanitized the knife using a 10% bleach solution between each sample and froze samples at − 20 °C before processing. At each sampling point, we also measured, to the nearest centimeter, the depth of the litter, fermentation, and humus layers (LFH layer). The LFH layer comprises the organic (O) horizon that overlies the uppermost mineral soil (A horizon).

To assess the concentration of mineral soil nutrients (phosphorus, ammonium, nitrate, calcium, iron, potassium, magnesium, manganese, effective cation exchange capacity, base saturation, and sodium) and pH, we sampled soils to 10 cm in a semi-random grid across the entire UFDP (Additional file 2). Soil nutrient concentrations were measured following the analytical methods of Baldeck et al. (2013). Non-nitrogen nutrients were extracted using a Mehlich III solution and analyzed using an atomic emission-inductively coupled plasma (AE-ICP, Perkin Elmer Inc., MA, USA). Nitrogen was extracted as NH_4^+ and NO_3^- with a 2 M KCI solution and analyzed using an auto-analyzer (OI FS 3000, OI Analytical, College Station, TX, USA).

Sample preparation

To prepare soil samples for DNA extraction, we thawed each sample and sieved them through progressively finer sieves up to 2 mm to remove fibrous organic matter. We bleached and dried sieves between each sample to avoid

Fig. 3 Images from the sampling area at the Utah Forest Dynamics Plot, Utah, USA. **a** A view to the southwest from the sampling area. **b** A view to the east from the sampling area. **c** A view to the south from immediately above the sampling area. **d** A view to the northwest from within the sampling area. The dominant tree across all pictures is *Pinus longaeva* (Great Basin bristlecone pine)

cross-contamination. We freeze-dried samples until they had reached a stable weight. We pulverized freeze-dried samples to a fine powder using a Tissuelyser 2 (Qiagen, Hilden, Germany) and used MoBio DNeasy PowerSoil Kits (Qiagen, Hilden, Germany) to extract DNA following the manufacturer's instructions. After extraction of DNA, we iteratively amplified and visualized the DNA using gel-electrophoresis (Additional file 2).

Sequencing of fungal rDNA

We used MiSeq sequencing targeting the ITS2 region of fungal rDNA using fITS7 (Ihrmark et al. 2012) and ITS4 (White et al. 1990) primers. We amplified extracted rDNA through a two-step polymerase chain reaction (PCR). We ran the first PCR using 25 µL sample volumes with 2.5 µL DNA template, 7.8 µL water, 12.5 µL Platinum SuperFi PCR MasterMix (Thermo Fisher Scientific, Waltham, USA), 0.125 µL Bovine Serum Albumin, and 1 µL of each of the forward and reverse primers (95 °C for 3 min; 95 °C for 30 s, 50 °C for 1 min, 72 °C for 30 s, 35 cycles; and 72 °C for 10 min). The samples were pooled and cleaned using Sera-Mag Select beads (GE Healthcare, Chicago, USA) and washed in two 80% ethanol washes. We used Nextera Index primers with N7 (N5) for the forward (reverse) reads for the second PCR. For the second PCR, a 25 µL volume was used with 5 µL of water, 12.5 µL of Platinum SuperFi PCR MasterMix, 2.5 µL N7xx primers, 2.5 µL N5xx primers, and 2.5 µL DNA template (95 °C for 3 min; 95 °C for 30 s, 55 °C 30 s, 72 °C for 30 s, 72 °C for 5 min, for 8 cycles). Sequencing was conducted at the University of Alberta Molecular Biological Sciences Unit, with a MiSeq sequencing platform.

Bioinformatics

We denoised, quality-checked, and quality filtered the demultiplexed sequences in the R package dada2 1.18.0 (Callahan et al. 2016) to create amplicon sequence variants (ASV). We filtered sequences to remove those with ambiguous bases and limited the maximum number of expected errors to two per sequence. Following identification and removal of chimeric sequences (Additional file 1: Table S2), we assigned taxonomy from the UNITE database (Nilsson et al. 2019) with the IDTAXA function in the DECIPHER 2.18.1 R package (Wright 2016).

After assigning taxonomy, we analyzed the results using the phyloseq 1.38.0, vegan 2.5-7, ggplot2 3.3.5, and ggpubr 0.4.0 R packages (McMurdie and Holmes 2013; Wickham 2016; Oksanen et al. 2020; Kassambara 2020). We had several duplicated samples that were amplified as safeguards against the loss of low-quality samples. In four cases the duplicates and originals were successfully amplified. We merged the duplicate samples by averaging sequence abundance. After merging, we visualized the distribution of sequence abundance and rarefied to 12,500 sequences to account for uneven sampling depth (Additional file 3: Fig. S1). We removed four samples that were below the 12,500-sequence cutoff.

To assign functional guilds to ASV, we used the FUNGuild database (Nguyen et al. 2016a), which assigns functional guilds to fungi based on the taxonomic assignment of the sequence. Common guilds include "Ectomycorrhizal", "Saprotrophic", or some combination of guilds as in "Ectomycorrhizal–Saprotrophic" when fungi are capable of existing across multiple functional guilds. Because of unknown or unresolved taxonomic assignments, many ASVs are classed as having an 'Unknown' guild. Additionally, many sequences are assigned to multiple potential guilds and were classified as 'Mixed EM' if one of the potential guilds was ectomycorrhizal. We included mixed guilds within the Saprotrophic classification if they included at least one known saprotrophic function, i.e., "wood–saprotroph–ectomycorrhizal".

Analyses

We used kriging to interpolate measurements of pH, LFH depth, and soil nutrients, across our sampling area. We used the 'powerTransform' function from the car 3.0-7 R package (Fox and Weisberg 2018) to normalize the variables. After transformation, we excluded nitrate and base saturation, which were still strongly non-normal. We generated semivariograms for each normalized variable and assessed the spatial autocorrelation of each. We used the 'krige' function to interpolate the remaining measurements and then transformed each nutrient to their original units (mg kg^{-1}) for analysis (Additional file 3: Fig. S2). For the LFH, we included an additional 160 depth measurements of LFH ($n_{total} = 295$) that were taken across the sampling area (Lutz et al. 2021a).

To assess spatial autocorrelation of fungal communities and functional guilds we used the 'mantel.correlog' function to plot mantel correlograms with 999 permutations (McMurdie and Holmes 2013). Distances were constructed using Euclidean distances between sampling locations. After assessing the entire fungal community, we split apart the fungal dataset into ectomycorrhizal and saprotrophic guilds and ran separate correlograms of each guild's community.

To compare the spatial autocorrelation of belowground fungi with aboveground trees and deadwood, we assessed the spatial autocorrelation of all living trees and mapped deadwood. Deadwood biomass calculations were conducted using the R packages rgdal version 1.4-8, rgeos version 0.5-2, sp version 1.3-2, and sf version 0.8-1 (Pebesma and Bivand 2005; Pebesma 2018; Bivand et al. 2019a, b). To assess the spatial autocorrelation of living trees, we binned trees within 5×5 m cells and summed

the basal area, by species, within each cell. After binning trees, we calculated the basal area of each tree species and standardized the community dataset using a Hellinger transformation. After standardization, we detrended the tree data using a linear regression against the centroid coordinates of each cell. Finally, we calculated the Euclidean distance of the regression residuals to calculate the mantel correlogram for the tree community.

To assess the spatial autocorrelation of deadwood, we calculated the biomass of all mapped deadwood (Additional file 2). We aggregated piece-level values of deadwood biomass within 5×5 m cells divided across the 1.15-ha sampling area. For pieces that lay across cell boundaries, we virtually separated them into new fragments, each wholly contained in a single cell. After summation, we standardized the dataset with a Hellinger transformation, detrended the data using a linear regression, and calculated the Euclidean distance of the regression residuals to calculate the mantel correlogram for deadwood.

We used the "specaccum" function in the vegan 2.5-7 R package to generate species accumulation curves by fungal guilds (Oksanen et al. 2020). We calculated Shannon's diversity using the 'estimate_richness' function in the R package phyloseq 1.38.0, on un-rarefied community data (McMurdie and Holmes 2013).

To assess the influence of soil nutrients on fungal community richness, we aggregated nutrients using a principal coordinate analysis with a correlation matrix to collapse nutrients into a primary and secondary component which collectively explained 82.7% of the variation within nutrients (Additional file 1: Table S3, Additional file 3: Fig. S3).

To assess the influence of aboveground forest structure, nutrients, and topography on the total and guild-specific communities, we used a permutational analysis of variance (PERMANOVA) with 999 permutations. We derived elevation from 0.5×0.5 m LiDAR (UGRC 2018), with landscape profile curvature calculated using ArcGIS 10.7 (ESRI, Redlands, CA, USA). To characterize the tree and snag community around each sample, we selected the maximum extent of their spatial autocorrelation of each fungal community (e.g., total, ectomycorrhizal, saprotroph) as a buffer in which to assess aboveground tree, snag, and downed wood characteristics. We calculated the basal area of all trees and snags and weighted each by the distance from the sampling location before summing the basal area, by tree and snag species. For deadwood, we summed the biomass of each species of deadwood within the specific extent of the sample. Finally, we retrieved the point-estimates of the nutrient principal components, LFH depth, landscape curvature, and elevation for each sample.

We used a random forest model to identify key aboveground factors influencing belowground fungal richness. We chose a random forest model as it accommodates non-normal data and can assess non-linear relationships between the dependent and independent variables. We used the randomForest 4.6–1.4 R package (Liaw and Wiener 2002) and ran separate random forest models for total, ectomycorrhizal, and saprotrophic community richness. With richness as our dependent variable, we tested both the identity and distance of the nearest tree and nearest large-diameter tree (>40.2 cm DBH), by tree species, as our independent variables. The 40.2 cm DBH threshold (Additional file 3: Fig. S4) was selected as an a priori threshold as it is the diameter in the UFDP above which trees contain half of the aboveground biomass (Lutz et al. 2018) and this metric can thus be used to set similar thresholds for large-diameter trees in other forests. In all models, we included the first two nutrient components derived from a principal component analysis (PCA), as well as elevation, LFH depth, and landscape curvature as abiotic covariates. We used the 'randomForest' function with 999 trees (Liaw and Wiener 2002) and default settings for the number of splits. We plotted partial dependence plots for each variable and graphed the increase in mean square error (MSE) for each variable.

Statistical analyses were conducted within the R Studio 2021.09.1 interface for R 4.2.1 (R Core Team 2020; R Studio Team 2021).

Results

Fungal composition, richness, and function

After dada2 quality control, we had 2,305,722 sequences from 126 samples with a mean sequence length of 309 ± 3.5 bases (SE). After rarefaction and merging of duplicate samples, we had 117 samples and found 6,177 fungal ASVs with a mean of 155 ± 5 ASVs per sample (Additional file 3: Fig. S5). Mean Shannon's diversity was 4.0 ± 0.0 with a range of 2.7–4.9 per sample. A total of 2207 ASVs (35.7%) representing 13.4% of sequences were not assigned a taxonomic level of Phylum or below. Species accumulation curves indicate that we sampled >90% of the fungal community and that 99 samples were needed to sample 90% of all ASVs (Additional file 3: Fig. S6). Ascomycota represented 52.1% of all sequences and had 2003 ASVs. In contrast, Basidiomycota represented 31.6% of all sequences and 1,446 ASVs. The most read-abundant ASVs were within the ectomycorrhizal genera of *Inocybe*, *Wilcoxina*, *Tricholoma*, *Geopora*, and *Sebacina* (Fig. 4). The largest single functional guild was ectomycorrhizal (597 ASVs; 25.5% of sequences) while 4349 ASVs (70.4%) representing 54.8% of sequences were not assigned a functional guild (Additional file 1: Table S4). Fungi capable of acting as saprotrophs accounted for 956 ASVs and

12.9% of total sequences. The most read-abundant ASVs representing saprotrophs were unidentified fungi within the Thelephoraceae and Pseudeurotiaceae families.

Spatial autocorrelation of fungi, trees, and deadwood

Within the sampling grid, composition of the entire fungal community showed weak spatial autocorrelation at distances from 4.5 m to 5.8 m (Fig. 5a). In contrast, ectomycorrhizal fungal communities showed consistent autocorrelation from 0.6 to 16.1 m (Fig. 5b). Similarly, saprotrophic fungal communities had spatial autocorrelation from 0.6 to 19.9 m (Fig. 5c). Both forest tree composition and deadwood biomass were positively autocorrelated from 0.6 to 30.5 m (Additional file 1: Table S5, S6, S7). Negative spatial autocorrelation existed for both trees (> 30.0 m) and deadwood (> 30.5 m) (Additional file 1: Table S8, S9). The depth of the LFH was autocorrelated from 0.0 to 57.0 m (Additional file 3: Fig. S7) while tree age was autocorrelated at distances of 0.0–163.0 m across the entire 15.32 ha of the UFDP (Additional file 3: Fig. S8).

Influence of aboveground forest structure on fungal composition and richness

After identifying the maximum distance of spatial autocorrelation of each fungal guild, we used this value to test the distance-weighted influence of all tree species within each guilds' neighborhood. Total fungal community dissimilarity was associated with the distance-weighted basal area of living *P. tremuloides* and *R. cereum* within 6.0 m (Table 1). Ectomycorrhizal fungal community dissimilarity was associated with soil nutrients and living distance-weighted basal area of *A. bifolia* and *A. concolor* within 16.0 m. Finally, saprotrophic fungal community dissimilarity was associated with soil nutrients, depth of the LFH layer, elevation, living distance-weighted basal area of *P. longaeva*, *P. menziesii*, and *R. cereum* along with dead distance-weighted basal area of *A. bifolia* and *P. tremuloides* within 20.0 m (Table 1). Random forest models testing the influence of the nearest tree and nearest large-diameter tree varied substantially, by fungal guild, in their variation explained. Total fungal richness was better explained by models with distance to the

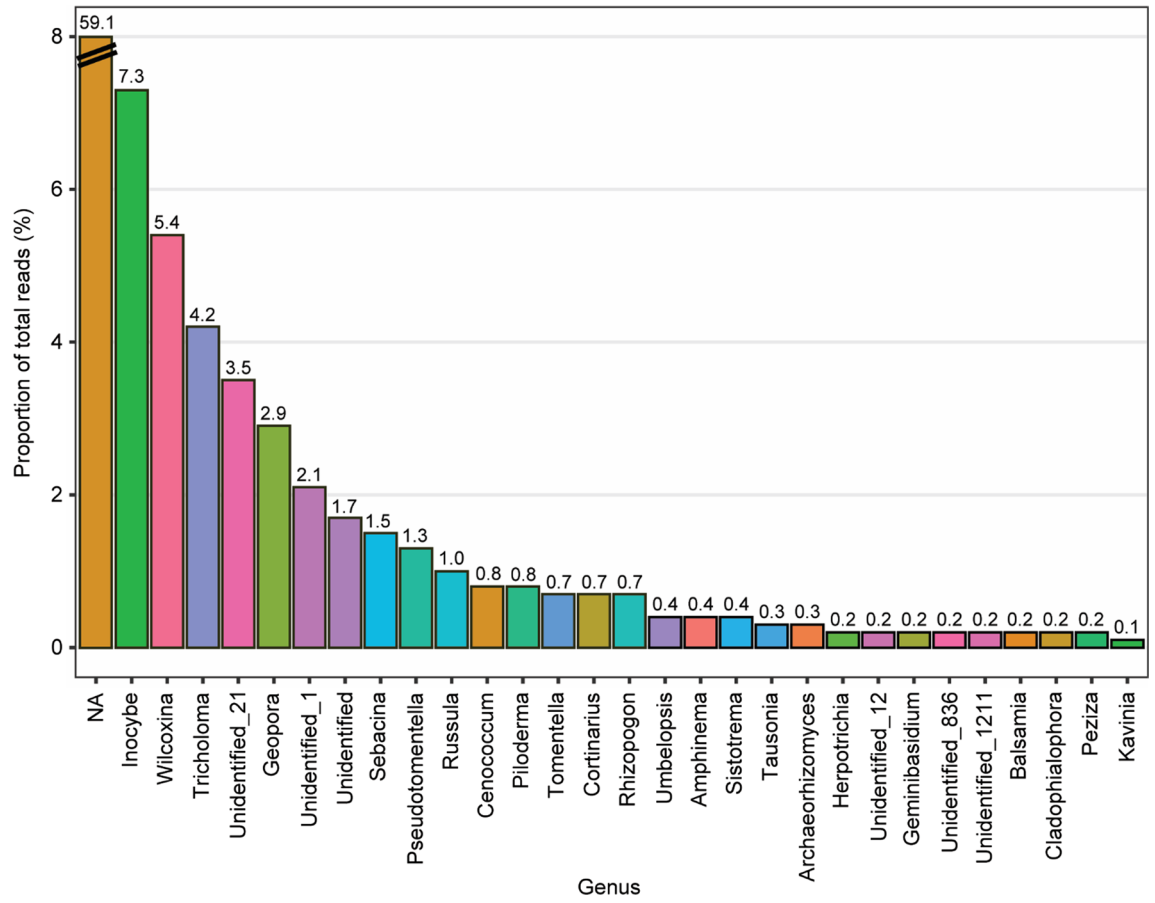

Fig. 4 The total proportional read abundance for the 30 most read-abundant fungal genera within the Utah Forest Dynamics Plot, Utah, USA

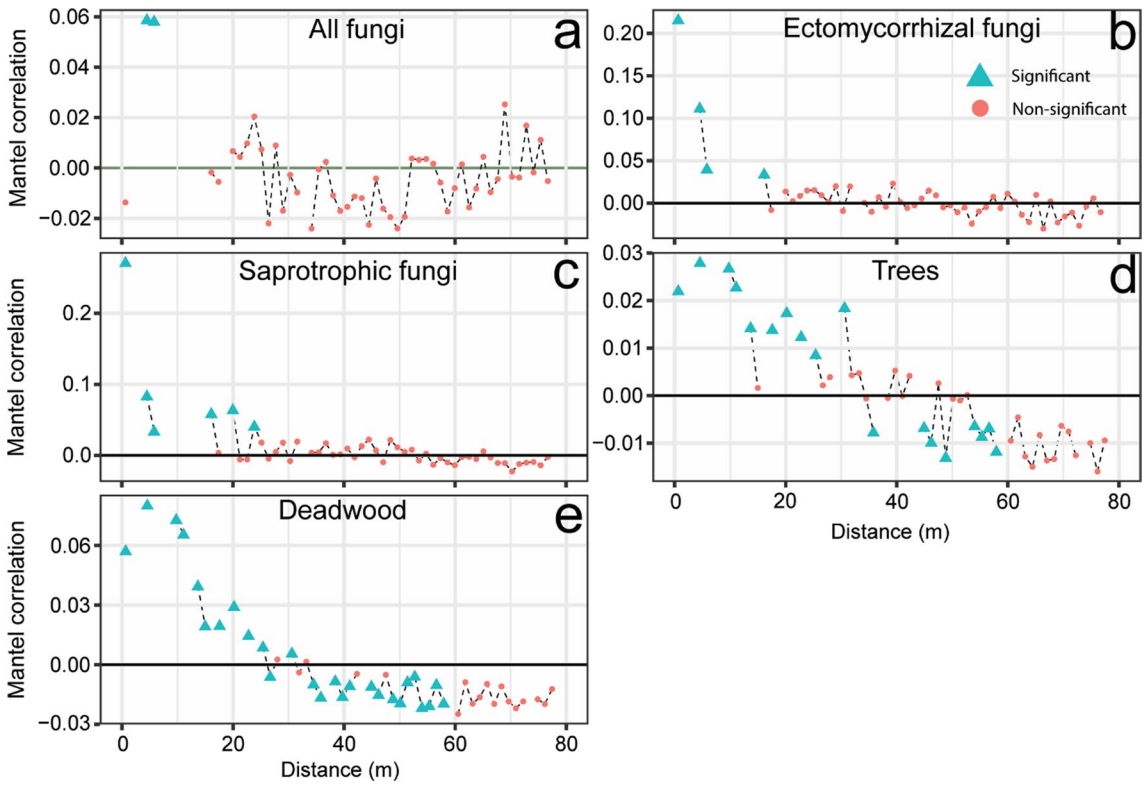

Fig. 5 The spatial autocorrelation of **a** all fungi, **b** ectomycorrhizal fungi, **c** saprotrophic fungi, **d** live-trees, and **e** deadwood at the Utah Forest Dynamics Plot, Utah, USA

nearest large-diameter tree (10.4% variation explained) than by models with distance to the nearest tree (9.5%). The variables with the greatest increase in mean square error, a measure of variable importance, were distance to the nearest large-diameter dead *A. bifolia*, large-diameter living *P. flexilis*, and large-diameter living *P. engelmannii* (Additional file 1: Table S10). Partial dependency plots indicate that fungal richness was higher by nearby (0–20 m) large-diameter dead *A. bifolia*, depressed near large-diameter live *P. flexilis* (0–20 m), and large-diameter living *P. engelmannii* (0–20 m) (Additional file 3: Fig. S9).

Ectomycorrhizal fungal richness was better explained by distance to the nearest large-diameter tree (38.7% of variation explained; Fig. 6) than by distance to the nearest tree (34.7%). Fungal richness increased at close distances (0–25 m) to large-diameter living *P. engelmannii,* increased with increasing values of soil component 2, and was depressed at close distances (0–25 m) around large-diameter dead *P. engelmannii* (Fig. 6b). In contrast, saprotrophic fungal richness was poorly explained by distance to the nearest large-diameter tree (− 11.0%) and distance to the nearest tree (− 15.8%). The most important variables for saprotrophic fungal richness were distance to the nearest large-diameter live *A. bifolia,* elevation, and large-diameter dead *P. flexilis* (Additional file 3: Fig. S10).

Discussion

In support of our first and second hypotheses, we found that tree and belowground fungal communities were associated with one another and that specific aboveground variables were associated with ectomycorrhizal and saprotrophic fungal communities. Our third hypothesis was supported by the total and ectomycorrhizal fungal community richness, which had more variation explained by the nearest large-diameter tree than by the nearest tree. Cumulatively, our results highlighted a remarkably rich and unexplored fungal community that was associated with distinct abiotic and biotic variables operating at differing scales within the forest. Further research is needed to fully parse the mechanisms through which these variables influence fungal community composition and richness. However, our methods highlight the utility of pairing rigorous belowground sampling with spatially explicit tree and deadwood data.

Table 1 PERMANOVA output by fungal functional guild

	Total community	Ectomycorrhizal	Saprotrophic
Nutrients			
Component 1	0.10	**0.04**	**0.01**
Component 2	0.81	**0.01**	**0.01**
LFH	0.99	0.25	**0.01**
Topography			
Curvature	0.10	0.83	0.37
Elevation	0.26	0.14	**0.05**
Living trees			
Abies bifolia	0.44	**0.03**	0.07
Abies concolor	0.58	**0.01**	0.06
Picea engelmannii	0.05	0.09	0.37
Picea pungens	0.25	0.52	0.25
Populus tremuloides	**0.01**	0.20	0.25
Pinus flexilis	0.36	0.65	0.09
Pinus longaeva	0.58	0.28	**0.01**
Pseudotsuga menziesii	0.24	0.06	**0.01**
Juniperus communis	0.37	0.96	0.68
Ribes cereum	**0.01**	0.07	**0.04**
Dead trees			
Abies bifolia	0.78	0.21	**0.01**
Picea engelmannii	0.80	0.07	0.56
Picea pungens	0.54	0.28	0.08
Populus tremuloides	0.24	0.64	**0.01**
Pinus flexilis	0.57	0.52	0.23
Pinus longaeva	0.06	0.48	0.21
R^2	0.19	0.35	0.25

Significance was calculated using a PERMANOVA with 999 permutations and denoted ($p < 0.05$) with bolded text

Fungal guilds and forest neighbors: unique spatial patterns and associations

Composition of fungal communities responded to both forest composition, soil nutrients, and topography, though at different spatial scales. Both ectomycorrhizal and saprotrophic fungal communities were autocorrelated beyond 15 m, nearly threefold greater distance than the total community. The autocorrelation of the total community is similar, though greater, than the 2–3 m distances commonly associated with fungal species (Lilleskov et al. 2004; Boraks et al. 2021). In contrast, the spatial autocorrelation of ectomycorrhizal and saprotrophic fungal guilds was far greater, though many meters short of the spatial autocorrelation of the forest (30.0 m) and deadwood (30.5 m). One potential reason for the offset between spatial scales of the aboveground forest and belowground fungal guilds is that individual trees most strongly influence their immediate 2.0–10.0 m neighborhood at the UFDP (Furniss et al. 2017), a similar range to that of lateral rooting extent (3.0–14.6 m) in mature subalpine trees (Berndt and Gibbons 1958). While the tree community composition is autocorrelated to 30.0 m, each individual tree has an area of influence on the order of 0.0–10.0 m (Furniss et al. 2017).

The living and dead basal area of specific tree species was associated with both the composition and richness of each fungal guild. However, ectomycorrhizal fungal composition and richness were better explained by our data than were the entire or saprotrophic communities. Our results mirror other studies which have found that tree species more strongly influenced ectomycorrhizal fungi than saprotrophic fungi (Nguyen et al. 2016b; Chen et al. 2019). Interestingly, the current survey detected more than three times as many fungal ASVs compared to our previous, targeted root- and soil samples collected around *P. flexilis*, *P. longaeva*, and *P. menziesii* at the UFDP (Birch et al. 2021, 2022b). Because ectomycorrhizal fungal richness increases with aboveground diversity, particularly at the genus-level (Gao et al. 2013), the diverse forest within the 1.15 ha likely drives a portion of the high fungal richness.

Composition of ectomycorrhizal fungal communities were better explained by all models than was the total community. This is likely due to divergent responses to environmental variables across the various functional guilds that are obscured by the poor taxonomic resolution of the entire community. Of note, *P. longaeva* was not strongly associated with ectomycorrhizal fungal composition or richness, despite its dominance across our sampling area. Only the basal area of living *A. bifolia* and *A. concolor* were significant in explaining ectomycorrhizal fungal community composition. Because *P. longaeva* is widely dispersed in the 1.15 ha, the locally rare tree species, such as *A. bifolia*, or *A. concolor*, may be hosting fungal communities that are not well-suited for *P. longaeva*. Supporting this idea, the most important variables explaining ectomycorrhizal fungal richness were the distance to the nearest *P. engelmannii*, and soil nutrients. While *P. engelmannii* was once abundant in the forest, after a Curculionidae *Dendroctonus rufipennis* Kirby (spruce beetle) outbreak in the 1990s, they are present mainly at small diameters across the landscape and uncommon within the UFDP (DeRose and Long 2007). The current scarcity of *P. engelmannii* and its association with fungal richness, suggests that locally rare tree species are important for promoting belowground fungal diversity.

Decomposing the relationships of saprotrophic fungi and the aboveground forest

In all cases, the saprotrophic fungal community had less variation explained by the model variables than

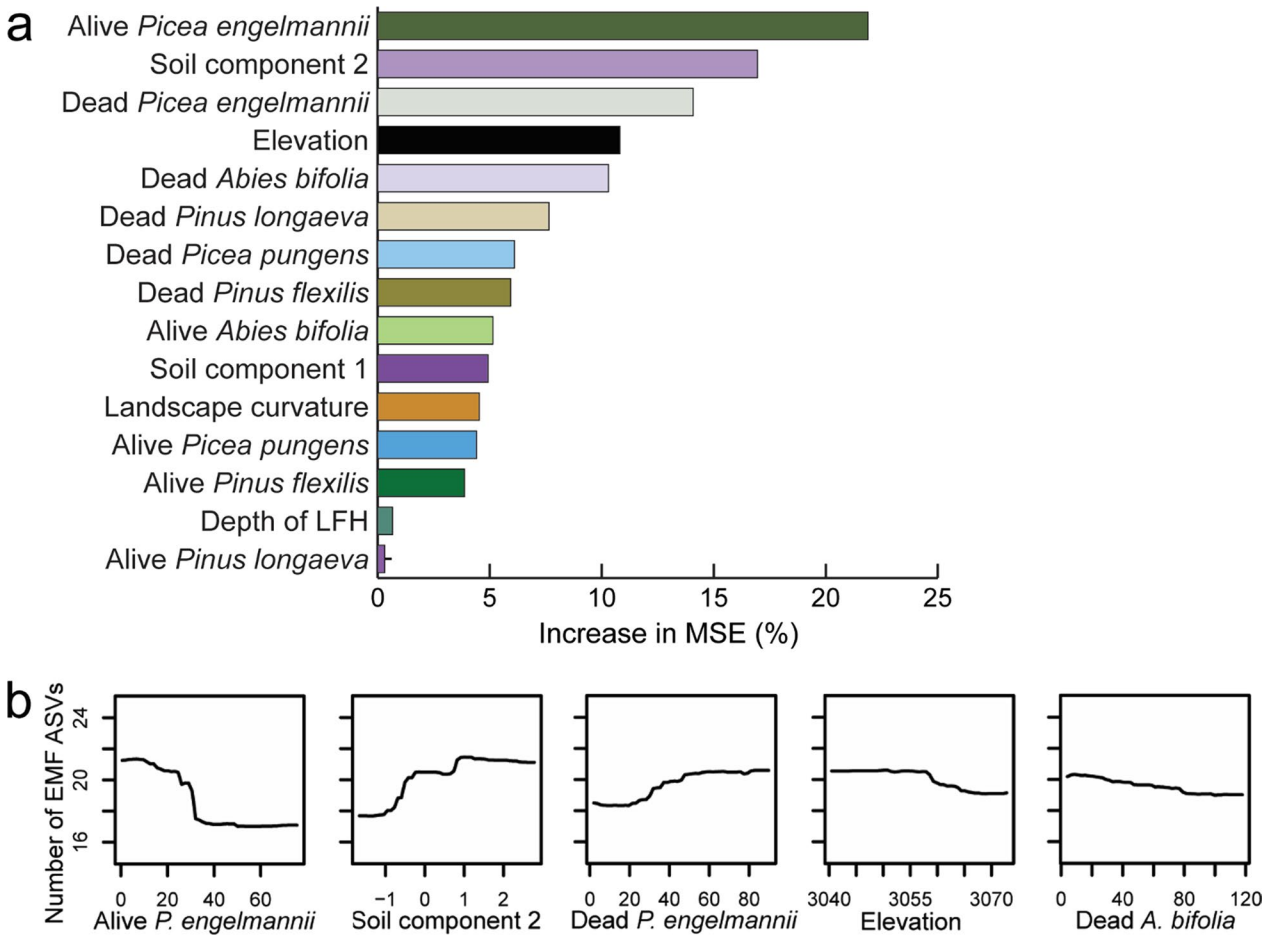

Fig. 6 The increase in mean square error (**a**) and partial dependence plots (**b**) from a random forest model assessing the influence of the nearest large-diameter (> 40.2 cm diameter at breast height) tree species on ectomycorrhizal fungal species richness at the Utah Forest Dynamics Plot, Utah, USA

did the ectomycorrhizal fungal community. Notably, the saprotrophic fungal composition was associated, in part, with living *P. longaeva*, the dominant tree species within the forest. Saprotrophic fungal composition was also influenced by the basal area of dead *A. bifolia* and *P. tremuloides.* Litter and wood from *A. bifolia* have a longer residence time than *Picea* wood (Bigler and Veblen 2011), while *P. tremuloides* likely decays faster than the other species (Angers et al. 2012). Thus, the differing residence times and parent material of the litter and deadwood may alter the surrounding saprotrophic communities. The turnover time for deadwood carbon has been estimated at being more than 580 years in similar forests (Kueppers et al. 2004), highlighting the enduring legacy of deadwood on saprotrophic communities and forest nutrients. Live and dead tree species were better predictors of saprotrophic richness than were soil nutrients or the depth of the LFH. This is surprising, as snags represent a relatively small (36 Mg ha^{-1}) component of the dead biomass within the UFDP with most (62 Mg ha^{-1}) provided by litter, duff, and deadwood (Lutz et al. 2021a). In addition to the differences in the size of biomass pools between snags and the LFH and deadwood pools, standing dead trees will have a lower root surface area in contact with the soil as a result of root decay and thus have a smaller portion of their biomass accessible to soil-associated saprotrophs.

While our saprotrophic-richness models included the depth of the LFH, a surrogate for saprotroph-available biomass, we did not characterize the relative contribution of each tree species litterfall to the standing LFH layer, which influences saprotrophic communities (Otsing et al. 2018). In general, microbes break down organic matter more quickly when it has low molecular diversity, low spatial heterogeneity, and when organic matter deposition occurs regularly (Lehmann et al. 2020). In

contrast, the UFDP has several tree species which differ in deadwood residence times by many orders of magnitude and has sporadic, high-volume deposition of woody material from bark-beetle outbreaks or fire every several centuries (Veblen et al. 1994). Constitutive defenses of wood vary widely among UFDP tree species (Runyon et al. 2020; Ott et al. 2021) and may drive known differences in dead wood residence time. The total amount of organic material present may have lesser importance for saprotrophic fungal diversity than its composition (i.e., variability in the types of plant litter deposited), which in turn influences the composition of the resulting organic matter and its physical and chemical stabilization in the soil matrix (Schmidt et al. 2011; Lehmann et al. 2020). Assessing these characteristics of the LFH layer and soil organic matter were beyond the scope of this study but represent directions for future research. The presence of living trees likely indicates the presence of local ectomycorrhizal fungi which may compete with saprotrophic fungi and thereby reduce the decomposition rates of soil organic matter (Gadgil and Gadgil 1971; Fernandez and Kennedy 2016). This apparent competition between ectomycorrhizal and saprotrophic fungi is variable between forests, but may further reduce the ability of saprotrophic fungi to access and decompose organic matter.

Soil nutrients were associated with compositional changes for ectomycorrhizal and saprotrophic fungal communities, but not for the entire fungal community, indicating different proclivities for soil nutrients across the full fungal community. The richness of all fungi was associated with soil component 2, which was correlated with higher manganese and potassium, and lower ammonium. Manganese peroxidase is used by white-rot fungi to decompose lignin (Berg et al. 2015) and is a limiting factor for saprotrophic fungi seeking to decompose organic material (Kranabetter 2019, 2021). Potassium is a key plant nutrient and ectomycorrhizal fungi can participate in both weathering and transport of potassium to plants in exchange for carbon (Dominguez-Nuñez et al. 2016). Finally, ammonium is a source of nitrogen, a critical nutrient for plants and fungi (Smith and Read 2010). Each of these nutrients could play a role in shaping specific fungal guilds depending on local resource limitations, at least as observed at the time of sampling.

Legacy of forest disturbances on soils, forests, and fungi

The structure and composition of the aboveground forest and the soil environment are a partial product of past disturbances. Disturbance to the overstory composition such as beetle-kill or fire can differentially select for or against certain tree species, thereby influencing the amount, time-scale, and chemistry of organic matter inputs to soil, which in turn provide the substrate for decomposition (Šťursová et al. 2014; Williams et al. 2016). The characteristics of these inputs also differ among disturbances; for example, beetle infestations may increase plant litter and deadwood. In contrast, fires can consume deadwood and LFH horizons, as well as organic matter in surface mineral soils (Miesel et al. 2018). Fires can also alter the soil physical environment (Quigley et al. 2019) and the composition of microbial communities (Adkins et al. 2020). Because tree size and age are closely related at the UFDP (Birch et al. 2021), the largest-diameter trees are likely to also be the oldest trees and have survived multiple disturbances. Thus, large-diameter trees at the UFDP may represent survival of tree roots through multiple disturbances over time, leading to greater diversity of soil organic matter and fungal communities.

Fungi and old trees: who selects whom?

Perhaps one of the most interesting questions raised by this and other studies of mycorrhizal fungal communities associated with old trees (Birch et al. 2021) is whether large, old trees create unique fungal communities, or whether specific fungal communities allow trees to persist to old ages and large sizes (Fig. 1). From one perspective, as trees become older, they may be able to be colonized by a more diverse fungal community as a function of random colonization over time. However, as trees age they may support co-evolved fungi that have adapted to late-successional forest conditions. Previous work at the UFDP found that deterministic selection overwhelmingly contributed to fungal community assembly (> 80%) on the roots and in soils around *Pseudotsuga menziesii* around our sampling area and that drift and dispersal limitations accounted for < 20% of community assembly (Birch et al. 2022b). This suggests that deterministic selection, either from bi-directional tree-fungi selection, or environmental filtering are likely the dominant factors influencing fungal community assembly.

Fungal communities become increasingly dissimilar to one another with tree age, even out to 1400 years old (Birch et al. 2021) and at least a portion of this is likely due to the effect of species richness (Jiang et al. 2021) or within-species genetic diversity (i.e., ploidy of *Populus*; Bishop et al. 2019). The age of the forest at the UFDP is a remnant signature of multiple fires and intermittent drought over the previous millennia that disturbed heterogeneous patches within the forest (Additional file 3: Fig. S8). A combination of size and age-related changes within trees are likely responsible for explaining the relationship between large trees and fungal richness. Likewise, specific fungal communities may also promote the health and persistence of large-diameter trees which in

turn promote forest structural heterogeneity (Lutz et al. 2013). Old-growth trees are of special conservation concern globally (Lindenmayer and Laurance 2016), and the preservation of large, old trees may help preserve unique belowground fungal communities. We used a large-diameter threshold above which trees contained half of the forest biomass which can be easily adapted to identify and test the influence of large-diameter trees in other forests (Lutz et al. 2018). Our results suggest that management actions that conserve large-diameter trees may be an effective way of promoting belowground ectomycorrhizal fungal richness, particularly if trees are spaced within 0.0–16.0 m. The exact density, species, and size of large-diameter trees which are associated with fungal community composition will likely vary by forest and requires further research. Management aimed at promoting structural diversity and deadwood retention has been previously linked with improved fungal richness (Dove et al. 2021; Tomao et al. 2020) and we expect that structurally complex forests will promote a variety of microhabitats and assembly processes that may improve fungal richness.

Conclusion

Hidden below an old-growth, globally unique forest was a diverse, largely unknown fungal community. Fungal functional guilds differed markedly in their spatial structure and the environmental variables explaining their composition and richness. These results highlight the utility of pairing spatially explicit tree and wood mapping with a rigorous sampling of belowground fungi. Of key importance, we found that the location and species of large-diameter trees were excellent predictors of ectomycorrhizal fungal richness and fair predictors of overall fungal richness. This work adds further evidence to the body of literature supporting the outsized ecological influence that large-diameter trees have on their ecosystems and the critical importance of conserving these vulnerable giants.

Abbreviations

ASV: Amplicon sequence variant; DBH: Diameter in centimeters at breast height (1.37 m); LFH: Litter–fermentation–humic layer; PCR: Polymerase chain reaction; UFDP: Utah Forest Dynamics Plot.

Supplementary Information

The online version contains supplementary material available at https://doi.org/10.1186/s13717-022-00415-8.

Additional file 1: Table S1. The basal area, number of stems, and range of ages for each of the woody species within the 1.15 ha forest sampled for fungal communities in Utah, USA. **Table S2**. The number of fungal sequences at each step of the DADA2 quality filtering pipeline. **Table S3**. The component loadings (Comp.1–Comp.5) of soil nutrients from a principal coordinate analysis at the Utah Forest Dynamics Plot, Utah, USA. **Table S4**. The proportional sequence abundance (%) and number of amplicon sequence variants (ASVs) for the fungal functional guilds within the Utah Forest Dynamics Plot, Utah, USA. **Table S5**. The Mantel correlation coefficients between distance and community composition of all fungi at the Utah Forest Dynamics Plot, Utah, USA. Bolded values are significant (p <0.05). **Table S6**. The Mantel correlation coefficients between distance and community composition of all ectomycorrhizal fungi at the Utah Forest Dynamics Plot, Utah, USA. Bolded values are significant (p <0.05). **Table S7**. The Mantel correlation coefficients between distance and community composition of all saprotrophic fungi at the Utah Forest Dynamics Plot, Utah, USA. Bolded values are significant (p <0.05). **Table S8**. The Mantel correlation coefficients between distance and community composition of tree biomass at the Utah Forest Dynamics Plot, Utah, USA. Bolded values are significant (p <0.05). **Table S9**. The Mantel correlation coefficients between distance and community composition of all deadwood biomass at the Utah Forest Dynamics Plot, Utah, USA. Bolded values are significant (p <0.05). **Table S10**. The rank of variables in the increase in mean square error, in Random Forest models for fungal diversity, by fungal guild, at the Utah Forest Dynamics Plot, UT, USA

Additional file 2. Methods for removal of PCR inhibitors, biomass calculation for deadwood, and sampling of soil nutrients.

Additional file 3: Figure S1. The distribution of fungal sequence count for soil samples taken at the Utah Forest Dynamics Plot, Utah, USA. The red horizontal line denotes the 12,500 sequence cutoff used to rarefy the sequence abundances. **Figure S2**. The interpolated mineral soil nutrients at the Utah Forest Dynamics Plot, Utah, USA. **Figure S3**. A principal coordinate analysis (PCA) of soil nutrients at the Utah Forest Dynamics Plot, Utah, USA. Soil nutrients were interpolated across the plot and the values at 117 sampling locations were used for this PCA. **Figure S4**. The diameter at breast height (1.37 m; cm) for all tree species with > 10 individuals at the Utah Forest Dynamics Plot, Utah, USA. **Figure S5**. The distribution of (**A**) observed fungal amplicon sequence variants (ASVs) and (**B**) Shannon's Alpha diversity for soil samples taken at the Utah Forest Dynamics Plot, Utah, USA. The red horizontal lines in each panel mark the mean value. **Figure S6**. The species accumulation curves for all fungal amplicon sequence variants (ASV) (a), ectomycorrhizal fungi (b), and saprotrophic fungi (c) at the Utah Forest Dynamics Plot, Utah, USA. **Figure S7**. A fitted variogram of the semi-variance of the depth of the LFH layer (litter + duff) from 295 measurements across the Utah Forest Dynamics Plot, UT, USA. **Figure S8**. The estimated age of the forest at the Utah Forest Dynamics Plot, Utah, USA. Tree age was estimated using kriging interpolation of 127 trees. **Figure S9**. The increase in mean square error (a) and partial dependence plots (b) from a random forest model assessing the influence of the nearest large (>40.2 cm diameter at breast height) tree species on total fungal species richness at the Utah Forest Dynamics Plot, Utah, USA. **Figure S10**. The increase in mean square error (a) and partial dependence plots (b) from a random forest model assessing the influence of the nearest large (>40.2 cm diameter at breast height) tree species on saprotrophic fungal species richness at the Utah Forest Dynamics Plot, Utah, USA.

Acknowledgements

We thank the staff of Cedar Breaks National Monument for their ongoing support of the Utah Forest Dynamics Plot. We thank Duane Loveland, Joy Birch, Maria Birch, Nike Birch, L. Birch, Raúl Ballesteros, Juan Villalba, Jelveh Tamjidi, Sophie Dang, and James Franklin for assisting with sample storage and processing. We thank the Natural Science and Engineering Council of Canada and the Utah Agricultural Experiment Station for their funding support for this project. The authors thank the field crews who gathered data, each individually acknowledged at http://ufdp.org. We thank the R Core Team and the countless individuals who contribute to the open-source statistical programs that make this work possible.

Author contributions

JDB conducted the survey. JDB, JAL, and JK designed and conducted the analysis. All authors contributed to synthesis and writing. All authors read and approved the final manuscript.

Funding
Funding was received from the Natural Science and Engineering Council of Canada to JK and the Utah Agricultural Experiment Station (Projects 1153, 1398 and 1423 to JAL) which has designated this as Journal Paper 9626.

Availability of data and materials
The datasets supporting the conclusions of this article are available at the Utah State University digital archives (https://doi.org/10.26078/06mv-p792) (Birch et al. 2022c). Tree age data are publicly available online at the International Tree Ring Data Bank as chronologies UT545, UT546, UT547, UT548, and UT556 (https://www.ncei.noaa.gov/products/paleoclimatology).

Declarations

Ethics approval and consent to participate
Not applicable.

Consent for publication
Not applicable.

Competing interests
The authors declare that they have no competing interests.

Author details
[1]Department of Plant, Soil and Microbial Sciences, Michigan State University, 1066 Bogue Street, East Lansing, MI 48824, USA. [2]Department of Wildland Resources and the Ecology Center, Utah State University, 5230 Old Main Hill, Logan, UT 84322-5230, USA. [3]Department of Renewable Resources, University of Alberta, 751 General Services Building, Edmonton, AB T6G 2H1, Canada.

Received: 14 October 2022 Accepted: 22 December 2022
Published online: 04 January 2023

References

Adkins J, Docherty KM, Gutknecht JLM, Miesel JR (2020) How do soil microbial communities respond to fire in the intermediate term? Investigating direct and indirect effects associated with fire occurrence and burn severity. Sci Tot Environ 745:140957. https://doi.org/10.1016/j.scitotenv.2020.140957

Anderson-Teixeira KJ, Herrmann V, Rollinson CR, Gonzalez B, Gonzalez-Akre EB, Pederson N, Alexander MR, Allen CD, Alfaro-Sánchez R, Awada T (2022) Joint effects of climate, tree size, and year on annual tree growth derived from tree-ring records of ten globally distributed forests. Glob Change Biol 28:245–266. https://doi.org/10.1111/gcb.15934

Angers VA, Drapeau P, Bergeron Y (2012) Mineralization rates and factors influencing snag decay in four North American boreal tree species. Can J for Res 42(1):157–166. https://doi.org/10.1139/x11-167

Baldeck CA, Harms KE, Yavitt JB, John R, Turner BL, Valencia R, Navarrete H, Davies SJ, Chuyong GB, Kenfack D (2013) Soil resources and topography shape local tree community structure in tropical forests. Proc R Soc B 280:20122532. https://doi.org/10.1098/rspb.2012.2532

Bauhus J (2009) Rooting patterns of old-growth forests: is aboveground structural and functional diversity mirrored belowground? In: Wirth C (ed) Old-growth forests. Springer, Berlin. https://doi.org/10.1007/978-3-540-92706-8_10

Berg B, Erhagen B, Johansson M-B, Nilsson M, Stendahl J, Trum F, Vesterdal L (2015) Manganese in the litter fall-forest floor continuum of boreal and temperate pine and spruce forest ecosystems—a review. Forest Ecol Manage 358:248–260. https://doi.org/10.1016/j.foreco.2015.09.021

Berndt HW, Gibbons RD (1958) Root distribution of some native trees and understory plants growing on three sites within ponderosa pine watersheds in Colorado. Rocky Mountain Forest and Range Experiment Station, USDA Forest Service, Fort Collins. CO.

Bigler C, Veblen TT (2011) Changes in litter and dead wood loads following tree death beneath subalpine conifer species in northern Colorado. Can J for Res 41(2):331–340. https://doi.org/10.1139/X10-217

Birch JD, Lutz JA, Turner BL, Karst J (2021) Divergent, age-associated fungal communities of *Pinus flexilis* and *Pinus longaeva*. Forest Ecol Manage 494:119277. https://doi.org/10.1016/j.foreco.2021.119277

Birch JD, Chikamoto Y, DeRose RJ, Manvailer V, Hogg EH, Karst J, Love DM, Lutz JA (2022a) Frost-associated defoliation in *Populus tremuloides* causes repeated growth reductions over 185 years. Ecosystems. https://doi.org/10.1007/s10021-022-00799-w

Birch JD, Lutz JA, Karst J (2022b) Dancing with Douglas-fir: determinism dominates fungal community assembly processes. J Ecol 110(8):1857–1870. https://doi.org/10.1111/1365-2745.13910

Birch JD, Lutz JA, Struckman S, Miesel J, Karst J (2022c) Data for gridding. Utah State University. https://doi.org/10.26078/06mv-p792

Bishop M, Furniss TJ, Mock KE, Lutz JA (2019) Genetic and spatial structuring of *Populus tremuloides* in a mixed-species forest of southwestern Utah, USA. West North Am Nat 79(1):63–71. https://doi.org/10.3398/064.079.0107

Bivand R, Keitt T, Rowlingson B, Pebesma E, Sumner M, Hijmans R (2019a) rgdal: Bindings for the geospatial data abstraction library. R package version 1:4–8. The Comprehensive R Archive Network (CRAN). https://CRAN.R-project.org/package=rgdal

Bivand R, Rundel C, Pebesma E, Stuetz R, Hufthammer K, Giraudoux P (2019b) rgeos: interface to geometry engine—open source ('GEOS'). R package version 0.5–2. The Comprehensive R Archive Network (CRAN). https://CRAN.R-project.org/package=rgeos

Boraks A, Plunkett GM, Doro TM, Alo F, Sam C, Tuiwawa M, Ticktin T, Amend AS (2021) Scale-dependent influences of distance and vegetation on the composition of aboveground and belowground tropical fungal communities. Microb Ecol 81(4):874–883. https://doi.org/10.1007/s00248-020-01608-4

Callahan BJ, McMurdie PJ, Rosen MJ, Han AW, Johnson AJA, Holmes SP (2016) DADA2: high-resolution sample inference from Illumina amplicon data. Nat Methods 13(7):581–583. https://doi.org/10.1038/nmeth.3869

Chen L, Swenson NG, Ji N, Mi X, Ren H, Guo L, Ma K (2019) Differential soil fungus accumulation and density dependence of trees in a subtropical forest. Science 366(6461):124–128. https://doi.org/10.1126/science.aau1361

Davies SJ, Abiem I, Salim KA, Aguilar S, Allen D, Alonso A, Anderson-Teixeira K, Andrade A, Arellano G, Ashton PS (2021) ForestGEO: understanding forest diversity and dynamics through a global observatory network. Biol Conserv 253:108907. https://doi.org/10.1016/j.biocon.2020.108907

DeRose RJ, Long JN (2007) Disturbance, structure, and composition: spruce beetle and Engelmann spruce forests on the Markagunt Plateau, Utah. Forest Ecol Manage 244(1):16–23. https://doi.org/10.1016/j.foreco.2007.03.065

Dominguez-Nuñez JA, Benito B, Berrocal-Lobo M, Albanesi A (2016) Mycorrhizal fungi: role in the solubilization of potassium. In: Meena VS, Maurya BR, Verma JP, Meena RS (eds) Potassium solubilizing microorganisms for sustainable agriculture. Springer, India. https://doi.org/10.1007/978-81-322-2776-2_6

Dove NC, Klingeman DM, Carrell AA, Cregger MA, Schadt CW (2021) Fire alters plant microbiome assembly patterns: integrating the plant and soil microbial response to disturbance. New Phytol 230(6):2433–2446. https://doi.org/10.1111/nph.17248

Fernandez CW, Kennedy PG (2016) Revisiting the 'Gadgil effect': do interguild fungal interactions control carbon cycling in forest soils? New Phytol 209(4):1382–1394. https://doi.org/10.1111/nph.13648

Fox J, Weisberg S (2018) An R companion to applied regression. Sage Publications, Thousand Oaks

Furniss TJ, Larson AJ, Lutz JA (2017) Reconciling niches and neutrality in a subalpine temperate forest. Ecosphere 8(6):e01847. https://doi.org/10.1002/ecs2.1847

Gadgil RL, Gadgil PD (1971) Mycorrhiza and litter decomposition. Nature 233(5315):133–133. https://doi.org/10.1038/233133a0

Gao C, Shi N-N, Liu Y-X, Peay KG, Zheng Y, Ding Q, Mi X-C, Ma K-P, Wubet T, Buscot F, Guo L-D (2013) Host plant genus-level diversity is the best predictor of ectomycorrhizal fungal diversity in a Chinese subtropical forest. Mol Ecol 22(12):3403–3414. https://doi.org/10.1111/mec.12297

Hanson CA, Allison SD, Bradford MA, Wallenstein MD, Treseder KK (2008) Fungal taxa target different carbon sources in forest soil. Ecosystems 11(7):1157–1167. https://doi.org/10.1007/s10021-008-9186-4

Harmon ME, Woodall CW, Fasth B, Sexton J (2008) Woody detritus density and density reduction factors for tree species in the United States: a synthesis. General Technical Report NRS-29. Northern Research Station, USDA Forest Service, Newton Square, PA

Ihrmark K, Bödeker I, Cruz-Martinez K, Friberg H, Kubartova A, Schenck J, Strid Y, Stenlid J, Brandström-Durling M, Clemmensen KE (2012) New primers to amplify the fungal ITS2 region—evaluation by 454-sequencing of artificial and natural communities. FEMS Microbial Ecol 82(3):666–677. https://doi.org/10.1111/j.1574-6941.2012.01437.x

Jiang F, Lutz JA, Guo Q, Hao Z, Wang X, Gilbert GS, Mao Z, Orwig DA, Parker GG, Sang W (2021) Mycorrhizal type influences plant density dependence and species richness across 15 temperate forests. Ecology 102(3):e03259. https://doi.org/10.1002/ecy.3259

Kassambara A (2020) ggpubr: 'ggplot2' based publication ready plots. R package version 0.4.0. The Comprehensive R Archive Network (CRAN). https://CRAN.R-project.org/package=ggpubr

Keane RE (2008) Biophysical controls on surface fuel litterfall and decomposition in the northern Rocky Mountains, USA. Can J For Res 38(6):1431–1445. https://doi.org/10.1139/X08-003

Kim D, Shin YH (2016) Spatial autocorrelation potentially indicates the degree of changes in the predictive power of environmental factors for plant diversity. Ecol Indi 60:1130–1141. https://doi.org/10.1016/j.ecolind.2015.09.021

Kranabetter JM (2019) Increasing soil carbon content with declining soil manganese in temperate rainforests: is there a link to fungal Mn? Soil Biol Biochem 128:179–181. https://doi.org/10.1016/j.soilbio.2018.11.001

Kranabetter JM, Philpott TJ, Dunn DE (2021) Manganese limitations and the enhanced soil carbon sequestration of temperate rainforests. Biogeochemistry 156(2):195–209. https://doi.org/10.1007/s10533-021-00840-5

Kueppers LM, Southon J, Baer P, Harte J (2004) Dead wood biomass and turnover time, measured by radiocarbon, along a subalpine elevation gradient. Oecologia 141(4):641–651. https://doi.org/10.1007/s00442-004-1689-x

Lehmann J, Hansel CM, Kaiser C, Kleber M, Maher K, Manzoni S, Nunan N, Reichstein M, Schimel JP, Torn MS, Wieder WR, Kögel-Knabner I (2020) Persistence of soil organic carbon caused by functional complexity. Nat Geosci 13(8):529–534. https://doi.org/10.1038/s41561-020-0612-3

Liaw A, Wiener M (2002) Classification and regression by randomForest. R News 2(3):18–22

Lilleskov EA, Bruns TD, Horton TR, Lee Taylor D, Grogan P (2004) Detection of forest stand-level spatial structure in ectomycorrhizal fungal communities. FEMS Microbial Ecol 49(2):319–332. https://doi.org/10.1016/j.femsec.2004.04.004

Lindenmayer DB, Laurance WF (2016) The unique challenges of conserving large old trees. Trends Ecol Evol 31:416–418. https://doi.org/10.1016/j.tree.2016.03.003

Lutz JA (2015) The evolution of long-term data for forestry: large temperate research plots in an era of global change. Northwest Sci 89(3):255–269. https://doi.org/10.3955/046.089.0306

Lutz JA, Larson AJ, Freund JA, Swanson ME, Bible KJ (2013) The importance of large-diameter trees to forest structural heterogeneity. PLoS ONE 8(12):e82784. https://doi.org/10.1371/journal.pone.0082784

Lutz JA, Furniss TJ, Johnson DJ, Davies SJ, Allen D, Alonso A, Anderson-Teixeira KJ, Andrade A, Baltzer J, Becker KML, Blomdahl EM, Bourg NA, Bunyavejchewin S, Burslem DFRP, Cansler CA, Cao K, Cao M, Cárdenas D, Chang L-W, Chao K-J, Chao W-C, Chiang J-M, Chu C, Chuyong GB, Clay K, Condit R, Cordell S, Dattaraja HS, Duque A, Ewango CEN, Fischer GA, Fletcher C, Freund JA, Giardina C, Germain SJ, Gilbert GS, Hao Z, Hart T, Hau BCH, He F, Hector A, Howe RW, Hsieh C-F, Hu Y-H, Hubbell SP, Inman-Narahari FM, Itoh A, Janík D, Kassim AR, Kenfack D, Korte L, Král K, Larson AJ, Li Y, Lin Y, Liu S, Lum S, Ma K, Makana J-R, Malhi Y, McMahon SM, McShea WJ, Memiaghe HR, Mi X, Morecroft M, Musili PM, Myers JA, Novotny V, de Oliveira A, Ong P, Orwig DA, Ostertag R, Parker GG, Patankar R, Phillips RP, Reynolds G, Sack L, Song G-ZM, Su S-H, Sukumar R, Sun I-F, Suresh HS, Swanson ME, Tan S, Thomas DW, Thompson J, Uriarte M, Valencia R, Vicentini A, Vrška T, Wang X, Weiblen GD, Wolf A, Wu S-H, Xu H, Yamakura T, Yap S, Zimmerman JK (2018) Global importance of large-diameter trees. Glob Ecol Biogeogr 27(7):849–864. https://doi.org/10.1111/geb.12747

Lutz JA, Struckman S, Furniss TJ, Cansler CA, Germain SJ, Yocom LL, McAvoy DJ, Kolden CA, Smith A, Swanson ME (2020) Large-diameter trees dominate snag and surface biomass following reintroduced fire. Ecol Process 9:41. https://doi.org/10.1186/s13717-020-00275-0

Lutz JA, Struckman S, Furniss TJ, Birch JD, Yocom LL, McAvoy DJ (2021a) Large-diameter trees, snags, and deadwood in southern Utah, USA. Ecol Process 10:9. https://doi.org/10.1186/s13717-020-00275-0

Lutz JA, Struckman S, Germain SJ, Furniss TJ (2021b) The importance of large-diameter trees to the creation of snag and deadwood biomass. Ecol Process 10:28. https://doi.org/10.1186/s13717-021-00299-0

Maguire DA (1994) Branch mortality and potential litterfall from Douglas-fir trees in stands of varying density. Forest Ecol Manage 70(1–3):41–53. https://doi.org/10.1016/0378-1127(94)90073-6

McMurdie PJ, Holmes S (2013) phyloseq: an R package for reproducible interactive analysis and graphics of microbiome census data. PLoS ONE 8:e61217. https://doi.org/10.1371/journal.pone.0061217

Miesel J, Reiner A, Ewell C, Maestrini B, Dickinson M (2018) Quantifying changes in total and pyrogenic carbon stocks across fire severity gradients using active wildfire incidents. Front Earth Sci 6:41. https://doi.org/10.3389/feart.2018.00041

Nguyen NH, Song Z, Bates ST, Branco S, Tedersoo L, Menke J, Schilling JS, Kennedy PG (2016a) FUNGuild: an open annotation tool for parsing fungal community datasets by ecological guild. Fung Ecol 20:241–248. https://doi.org/10.1016/j.funeco.2015.06.006

Nguyen NH, Williams LJ, Vincent JB, Stefanski A, Cavender-Bares J, Messier C, Paquette A, Gravel D, Reich PB, Kennedy PG (2016b) Ectomycorrhizal fungal diversity and saprotrophic fungal diversity are linked to different tree community attributes in a field-based tree experiment. Mol Ecol 25(16):4032–4046. https://doi.org/10.1111/mec.13719

Nilsson RH, Larsson K-H, Taylor AFS, Bengtsson-Palme J, Jeppesen TS, Schigel D, Kennedy P, Picard K, Glöckner FO, Tedersoo L (2019) The UNITE database for molecular identification of fungi: handling dark taxa and parallel taxonomic classifications. Nucleic Acids Res 47(D1):259–264. https://doi.org/10.1093/nar/gky1022

Oksanen J, Blanchet FG, Friendly M, Kindt R, Legendre P, McGlinn D, Minchin PR, O'Hara RB, Simpson GL, Solymos P, Stevens MHH, Szoecs E, Wagner H (2020) vegan: community ecology package. R package version 2.5–7. https://CRAN.R-project.org/package=vegan

Otsing E, Barantal S, Anslan S, Koricheva J, Tedersoo L (2018) Litter species richness and composition effects on fungal richness and community structure in decomposing foliar and root litter. Soil Biol Biochem 125:328–339. https://doi.org/10.1016/j.soilbio.2018.08.006

Ott DS, Fettig CJ, Munson AS, Runyon JB, Ross DW (2021) Physical and chemical characteristics of blue and *Engelmann spruce* relative to spruce beetle host selection and colonization. Forest Ecol Manage 479:118577. https://doi.org/10.1016/j.foreco.2020.118577

Pebesma EJ (2018) Simple features for R: standardized support for spatial vector data. R J 10(1):439–446. https://doi.org/10.32614/RJ-2018-009

Pebesma E, Bivand RS (2005) S classes and methods for spatial data: the sp package. R News 5(2):9–13

Quigley KM, Wildt R, Sturtevant BR, Kolka RK, Dickinson MB, Kern CC, Donner DM, Miesel JR (2019) Fuels, vegetation, and prescribed fire dynamics influence ash production and characteristics in a diverse landscape under active pine barrens restoration. Fire Ecol 15:5. https://doi.org/10.1186/s42408-018-0015-7

R Core Team (2020) R: A language and environment for statistical computing. Version 4.2.1. R Foundation for Statistical Computing, Vienna. https://www.r-project.org/

R Studio Team (2021) RStudio: Integrated Development for R. Version 2021.09.1. https://posit.co/downloads/

Rudawska M, Wilgan R, Janowski D, Iwański M, Leski T (2018) Shifts in taxonomical and functional structure of ectomycorrhizal fungal community of Scots pine (*Pinus sylvestris* L.) underpinned by partner tree ageing. Pedobiologia 71:20–30. https://doi.org/10.1016/j.pedobi.2018.08.003

Runyon JB, Gray CA, Jenkins MJ (2020) Volatiles of high-elevation five-needle pines: chemical signatures through ratios and insight into insect and pathogen resistance. J Chem Ecol 46(3):264–274. https://doi.org/10.1007/s10886-020-01150-0

Schmidt MW, Torn MS, Abiven S, Dittmar T, Guggenberger G, Janssens IA, Kleber M, Kögel-Knabner I, Lehmann J, Manning DA (2011) Persistence of

soil organic matter as an ecosystem property. Nature 478(7367):49–56. https://doi.org/10.1038/nature10386
Smith SE, Read DJ (2010) Mycorrhizal symbiosis. Academic Press, Cambridge
Štursová M, Šnajdr J, Cajthaml T, Bárta J, Šantrůčková H, Baldrian P (2014) When the forest dies: the response of forest soil fungi to a bark beetle-induced tree dieback. ISME J 8(9):1920–1931. https://doi.org/10.1038/ismej.2014.37
Tang J, Luyssaert S, Richardson AD, Kutsch W, Janssens IA (2014) Steeper declines in forest photosynthesis than respiration explain age-driven decreases in forest growth. Proc Natl Acad Sci 111(24):8856–8860. https://doi.org/10.1073/pnas.1320761111
Teste FP, Simard SW (2008) Mycorrhizal networks and distance from mature trees alter patterns of competition and facilitation in dry Douglas-fir forests. Oecologia 158(2):193–203. https://doi.org/10.1007/s00442-008-1136-5
Tomao A, Antonio Bonet J, Castaño C, de-Miguel S (2020) How does forest management affect fungal diversity and community composition? Current knowledge and future perspectives for the conservation of forest fungi. Forest Ecol Manage 457:117678. https://doi.org/10.1016/j.foreco.2019.117678
Veblen TT, Hadley KS, Nel EM, Kitzberger T, Reid M, Villalba R (1994) Disturbance regime and disturbance interactions in a Rocky Mountain subalpine forest. J Ecol 82(1):125–135. https://doi.org/10.2307/2261392
Utah Geospatial Resource Center (2018) Southern Utah LiDAR elevation database. https://gis.utah.gov/data/elevation-and-terrain/2018-lidar-southern-utah/. Accessed 31 Oct 2021
Vives-Peris V, de Ollas C, Gómez-Cadenas A, Pérez-Clemente RM (2020) Root exudates: from plant to rhizosphere and beyond. Plant Cell Rep 39(1):3–17. https://doi.org/10.1007/s00299-019-02447-5
Vogt KA, Vogt DJ, Palmiotto PA, Boon P, O'Hara J, Asbjornsen H (1995) Review of root dynamics in forest ecosystems grouped by climate, climatic forest type and species. Plant Soil 187(2):159–219. https://doi.org/10.1007/BF00017088
Wasyliw J, Karst J (2020) Shifts in ectomycorrhizal exploration types parallel leaf and fine root area with forest age. J Ecol 108(6):2270–2282. https://doi.org/10.1111/1365-2745.13484
White TJ, Bruns T, Lee S, Taylor J (1990) Amplification and direct sequencing of fungal ribosomal RNA genes for phylogenetics. PCR Protocol Guide Methods Appl 18(1):315–322. https://doi.org/10.1016/B978-0-12-372180-8.50042-1
Wickham H (2016) ggplot2: elegant graphics for data analysis. Springer, Heidelberg. https://doi.org/10.1007/97803031902427704
Williams CA, Gu H, MacLean R, Masek JG, Collatz GJ (2016) Disturbance and the carbon balance of US forests: a quantitative review of impacts from harvests, fires, insects, and droughts. Glob Planet Chang 143:66–80. https://doi.org/10.1016/j.gloplacha.2016.06.002
Wright ES (2016) Using DECIPHER v2.0 to analyze big biological sequence data in R. R J 8(1):352–359. https://doi.org/10.32614/RJ-2016-025

Publisher's Note

Springer Nature remains neutral with regard to jurisdictional claims in published maps and institutional affiliations.

Submit your manuscript to a SpringerOpen journal and benefit from:

- ► Convenient online submission
- ► Rigorous peer review
- ► Open access: articles freely available online
- ► High visibility within the field
- ► Retaining the copyright to your article

Submit your next manuscript at ► springeropen.com